

# Raman Airborne Spectroscopic Lidar (RASL) - Final Report

David N. Whiteman, Geary Schwemmer, Kurt Rush, NASA/GSFC  
Igor Veselovskii, Belay Demoz, Zhien Wang, UMBC  
Wayne Welch, Welch Mechanical Design  
Luis Ramos, SSAI  
Richard Rallison, Ralcon Development Labs

September 30, 2002

## **Abstract**

The Raman Airborne Spectroscopic Lidar (RASL) was developed under the first NASA Instrument Incubator Program for laboratory validation. RASL signifies a great increase in airborne remote sensing capability over existing sensors at greatly reduced cost. This document details the scientific drivers and development activities for RASL, the current status of the instrument as well as the outlook for future use in atmospheric sciences. The first water vapor measurements of RASL indicate that it possesses the anticipated measurement range and sensitivity validating earlier numerical modeling that predicted that RASL would offer up to an order of magnitude greater resolution than existing airborne lidar systems.

# Contents

<b>1</b>	<b>Introduction</b>	<b>3</b>
<b>2</b>	<b>Scientific Motivation</b>	<b>4</b>
2.1	Earth Science Enterprise Research Priorities	4
<b>3</b>	<b>Raman lidar background</b>	<b>5</b>
<b>4</b>	<b>The Proposed Airborne Scanning Raman Lidar using Holographic Optical Elements</b>	<b>6</b>
<b>5</b>	<b>Work Performed under Instrument Incubator Project</b>	<b>6</b>
5.1	Year 1	6
5.1.1	HOE manufacture and testing	7
5.2	Years 2 and 3	10
5.2.1	Raman Airborne Spectroscopic Lidar	11
5.2.2	Current airborne water vapor lidars	13
5.2.3	Comparison of LASE water vapor measurements and RASL simulation	14
5.2.4	System Design	17
5.2.4.1	Telescope	17
5.2.4.2	Optical detection system	19
5.2.4.3	Laser	20
5.2.4.4	Data acquisition system	23
5.2.4.5	Aircraft window	23
5.2.5	Validation of RASL technologies during IHOP	25
5.2.6	Final assembly and test - first RASL measurements	27
5.2.6.1	Water vapor mixing ratio	28
5.2.6.2	Aerosol scattering ratio, aerosol depolarization, cirrus cloud optical depth and extinction/backscatter ratio	30
5.2.6.3	Liquid water measurements	35
<b>6</b>	<b>Applications of RASL to other science questions</b>	<b>35</b>
6.1	Aerosol backscatter, extinction, depolarization measurements - TOMS	37
6.2	Fiber optics port - aerosol backscattering and extinction for GLAS and CALIPSO	37
6.3	CO <sub>2</sub> measurements	38
<b>7</b>	<b>The future for RASL - getting into the air</b>	<b>38</b>
<b>8</b>	<b>References</b>	<b>40</b>

# 1 Introduction

The Raman lidar is well established as a leading research tool in the study of numerous areas of importance in the atmospheric sciences. The Raman lidar has been used to study the passage of frontal systems [1], stratospheric aerosols due to volcanic eruptions [2], atmospheric temperature variations in cirrus clouds [3], long term variation of water vapor and aerosols at a mid-continental site [4], cloud liquid water [5], cirrus cloud optical properties [6], the influence of thin cirrus clouds on satellite retrievals of water vapor [7], hygroscopic growth of aerosols [8], cloud base height detection [9], multi-wavelength Raman lidar measurements of aerosols enabling remote characterization of aerosols [10] [21] and other topics. However, the use of Raman lidar in airborne systems has been limited [14] to mostly nighttime measurements of stratospheric ozone and temperature. There has never been an airborne Raman lidar that possessed a diurnal ability to measure water vapor mixing ratio, perhaps the most important parameter of the atmosphere determining severe storm development and a powerful component of the earth's radiation balance. This lack of airborne Raman lidar development has been in part due to the lower scattering cross section inherent in the Raman process. This fact has required that Raman lidars possess higher power aperture products than traditional elastic backscatter lidars necessitating larger systems.

In order to decrease the cost, complexity and weight of Raman lidar systems and to allow Raman lidar technology to be more easily adapted to airborne platforms, we were funded through the first NASA Instrument Incubator Program (IIP) to develop an airborne Raman lidar capable of measuring water vapor during the daytime and nighttime that would offer measurements of numerous other atmospheric parameters important for satisfying the goals of NASA's Earth Science Enterprise (ESE) measurements program. These parameters include aerosol backscatter, extinction and optical depth, cirrus cloud optical depth and equivalent particle radius, cloud liquid water, cloud droplet size and cloud droplet number density. In an effort to provide lightweight scanning capability in this instrument, we proposed the concept of basing RASL on a light-weight, holographic telescope. The holographic telescope also acts as a large diffraction grating opening up the possibility of performing high resolution spectroscopic measurements of various atmospheric constituents as well.

Therefore, in this document, we will detail 1) the original design concept of the RASL instrument based on a holographic telescope, 2) the resulting research that demonstrated that certain design changes would be required in order to best address Earth Science Enterprise measurement needs, 3) the final RASL instrument 4) laboratory based measurements demonstrating the capability of the newly developed instrument.

## **2 Scientific Motivation**

### **2.1 Earth Science Enterprise Research Priorities**

NASA's Earth Science Enterprise (ESE) has recently established several broad questions to focus the research strategies of the Enterprise. Among these questions are:

1. *How are global precipitation, evaporation, and the cycling of water changing?*
2. *How are variations in local weather, precipitation and water resources related to global climate variation?*
3. *How can weather forecast duration and reliability be improved by new space-based observations, data assimilation, and modeling?*

A quote from the ESE Strategic Plan helps to focus how these questions might be addressed by ground-based, airborne and spaceborne remote sensing: "The new challenge is that of relating the large-scale atmospheric circulation to the life cycle of mesoscale storms (e.g. hurricanes) and other severe weather systems (e.g. tornado-generating rainstorms), and then understanding how that relationship might change in a future climate. Another challenge is that of deriving quantitative precipitation predictions from weather forecasting models. Both topics are actually central objectives of the U.S. Weather Research Program (USWRP). Another potential source of observational data on the life cycle of mesoscale storms (principally over land) is the measurement of the 3-dimensional structure of atmospheric temperature, moisture and wind around storm cells."

The International H<sub>2</sub>O Project (IHOP) field campaign held May - June 2002 in Oklahoma was designed exactly to address the questions raised in the above quote from the ESE Strategic Plan. It constituted the largest field campaign ever mounted to study weather. Among the goals of IHOP were to improve quantitative precipitation forecasting (QPF)

and predictions of convection initiation (CI) by providing more detailed measurements of water vapor variability. The detailed process studies that are required to address these goals require advanced ground-based and airborne sensors; space borne sensors do not provide water vapor data with sufficient resolution to improve the understanding of the underlying physics involved in these processes. Therefore, IHOP deployed 6 research aircraft and a large array of ground-based sensors to accomplish its goals. Ground-based measurements acquired during IHOP by the Raman lidar group's Scanning Raman Lidar (SRL) using some technologies developed under this IIP will be shown later in this report. Airborne measurements of water vapor were acquired by 3 airborne water vapor DIAL (Differential Absorption Lidar) instruments involved in IHOP. However as we will show the Raman approach as used in RASL not only permits a water vapor lidar to be developed at greatly reduced cost to a DIAL sensor, but enables a large number of additional measurements to be made simultaneously as well. These other measurements include aerosol extinction/optical depth, cloud liquid water, cirrus cloud optical depth and particle radius provided a broader measurement suite of high priority ESE measurements than any other airborne sensor. A flight ready RASL would have contributed an unprecedented array of data products to the IHOP objectives.

### **3 Raman lidar background**

Raman scattering is a weak inelastic molecular scattering process. For atmospheric measurements using lidar, the scattering process involves using a laser to excite a molecule from its initial vibrational state to an intermediate virtual state from which it makes a radiative transition to the next highest vibrational state. This transition leaves the molecule in a higher energy state. The scattered photon is thus of lower energy than the incident photon. The energy difference between the incident and the scattered photon is determined by the energy level spacing of the vibrational states of the molecule. The vibrational energy level spacing is unique to the molecule under study thus the shift can be used as a signature for the presence of the molecule in the atmosphere.

Raman lidar systems are designed to detect the wavelength-shifted light from molecules in the atmosphere. Various quantities can be measured by using filters at the appropriate shifted wavelengths. These include water vapor

(3654  $\text{cm}^{-1}$ ), liquid water (3425  $\text{cm}^{-1}$ ), nitrogen (2329  $\text{cm}^{-1}$ ), oxygen (1555  $\text{cm}^{-1}$ ), carbon dioxide (1285  $\text{cm}^{-1}$ ), sulphur dioxide (1152  $\text{cm}^{-1}$ ), etc. This illustrates one of the advantages of the Raman lidar approach to atmospheric measurements: a single wavelength is transmitted into the atmosphere exciting shifts in a wide variety of molecules enabling many different measurements.

## **4 The Proposed Airborne Scanning Raman Lidar using Holographic Optical Elements**

The funded research was to develop a laboratory version of an optimized airborne Raman lidar. During the first year of the IIP activity we studied the use of a Holographic Optical Element (HOE) as the scanner/receiver element for the new lidar system. The successful use of such a device could potentially reduce the size and weight of the lidar by coupling into a single component of the system the dual functions of laser scanner and lidar receiving telescope. The resulting weight reduction could allow it to be much more easily adapted to aircraft platforms. The holographic element, acting as a large diffraction grating, would disperse the various Raman shifted signals spatially. An array of fiber optics could be used to choose the desired wavelengths with high spectral resolution. By multiplexing the fiber signals, this new approach to Raman lidar design could allow fewer detectors to be used for the measurements. These are the advantages that made this approach an attractive one to pursue for an airborne Raman system. However, the research that was undertaken during the first year of this IIP activity indicated that the HOE technology was not yet mature enough for use in an optimized airborne scanning Raman lidar.

## **5 Work Performed under Instrument Incubator Project**

A summary will now be given of the work performed year by year during this IIP activity.

### **5.1 Year 1**

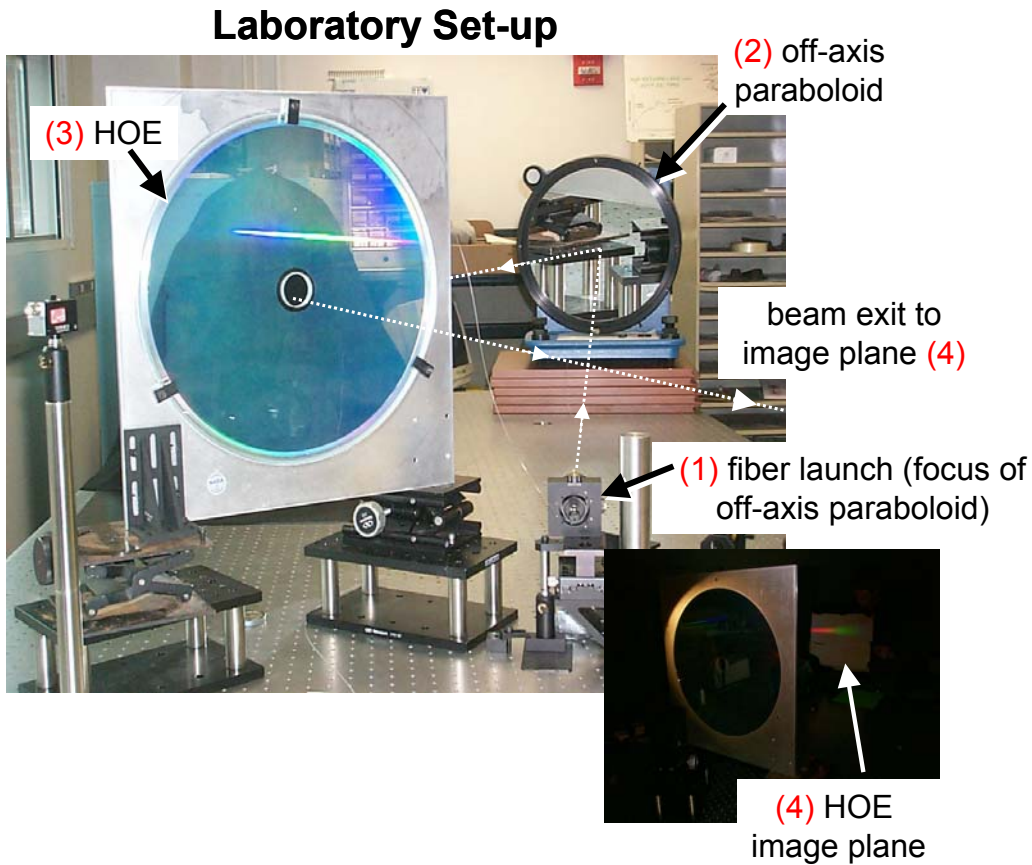


Figure 1: HOE test setup in the Raman lidar laboratory. The optical beam path and the sequence of surfaces for the measurements is shown.

#### 5.1.1 HOE manufacture and testing

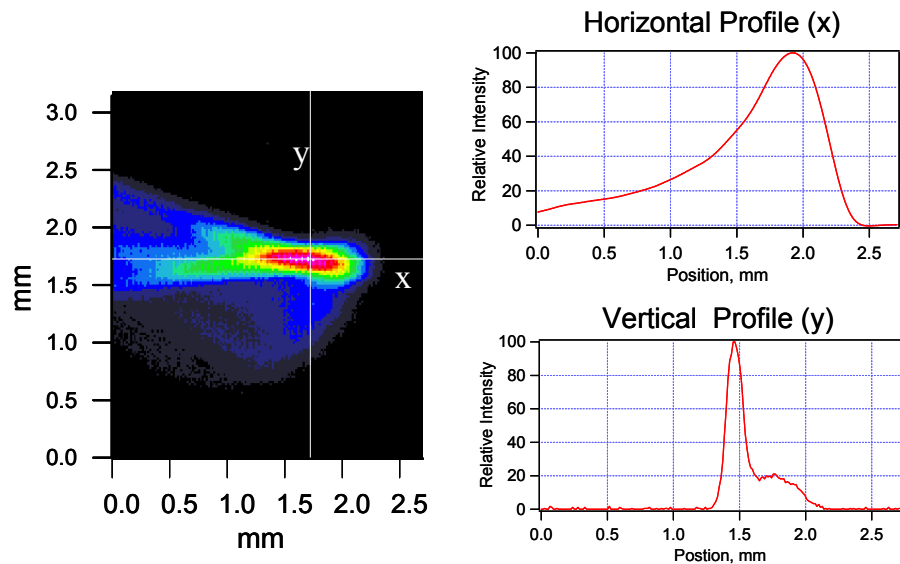
During the first year of this IIP effort, a 16" prototype HOE element for use in a Raman lidar system was designed, constructed and tested at NASA/GSFC. The goal was to produce an HOE that could, within a relatively short focal length, focus the Rayleigh-Mie backscattered signal as well as the Raman shifted signals over a  $\sim 70$  nm bandwidth with sufficient quality to permit sub-Angstrom resolution measurements over that spectral range. This would permit fibers to be located along the focal plane permitting any of these signals to be directed to the light sensing detector.

The HOE that was fabricated is shown in figure 1. The summary of the test results on this HOE are provided in the table below.

Wavelength (nm)	408	387	355
Incidence angle for maximum diffracted power (degrees)	33.3	33.3	33.3
Diffraction efficiency at 33.3 degrees (%)	32.7	41.4	31.3
Diffraction efficiency at 40 degrees (%)	66.4	60.0	67.3
Focal length at 33.3 degrees (mm)	2237	2362	2594
Focal length at 40 degrees (mm)	2252	2375	2613
Spot size (at 50% power) at 33.3 degrees (mm)	1.52	1.37	1.36
Spot size (at 50 % power) at 40 degrees (mm)	0.90	0.87	
Spot size (at 87% power) at 33.3 degrees (mm)		2.79	2.45
Spot size (at 87% power) at 40 degrees (mm)	1.56	1.47	
<i>Results of optical testing of the HOE for use in Raman lidar</i>			

From the table, one can see that signals at different wavelengths are focussed to spots of varying focal length. This is due to the natural dispersion of the HOE materials. These spots fall along a line that intersects the optical axis of the HOE but is not perpendicular to it. Also, the table indicates that the maximum diffraction efficiency and the minimum spot sizes are not achieved at the same incidence angle. The design goal, and the optical modeling of the HOE, both indicated that the maximum diffraction efficiency and the minimum spot size would occur at the same angle of 40 degrees. Therefore the actual HOE differed from the prediction of the optical ray trace model and necessitated a trade off between optical efficiency and resolution. Furthermore, the minimum spot size achieved in the actual HOE was considerably larger than that predicted by the optical model. An example of the spots measured for the HOE is shown in figure 2.

The ray trace model predicted 50 micron spot sizes, which translates into  $\sim 0.15$  Angstrom resolution. However, the 50 micron spot size corresponds to 25 micro-radian field of view of the telescope. The minimum desired field of view for making atmospheric measurements was 250 micro-radians implying that 1.5 Angstroms was the minimum useful resolution of the system and that 500 microns was the minimum useful spot size. These are acceptable numbers for a very useful Raman lidar since the typical spectral bandpass desired for the receiver system is  $\sim 3\text{\AA}$  in the water vapor channel at 408 nm. However, as shown in the table of HOE measurement results, the minimum spot size measured at 408 nm was actually 900 microns or more than an order of magnitude larger than the ray trace model. And this was achieved at 40 degree incidence angle, which was not the angle of maximum diffraction efficiency. In order to achieve



Example Spot Size measurement (408 nm, 33 deg.)

Figure 2: HOE spot size measurement made for the water vapor wavelength of 408 nm at an angle of 33 degrees.

the maximum diffraction efficiency, 33.3 degrees incidence angle was required implying that the minimum spot size was 1.52 mm at 408 and that the minimum useful field of view would be 0.75 milliradians. This large field of view would prevent daytime operations from occurring with the HOE due to insufficient suppression of daytime skylight.

Therefore the optical testing of the HOE indicated that in terms of focus quality and resolution it would not be able to meet the requirements of an optimized daytime/nighttime Raman water vapor lidar without auxiliary focussing lenses. Furthermore, there were mechanical complexities introduced by enabling scanning of the off-axis Raman signals. A 0.4 m aperture HOE was produced during the first year of this activity with a ~2 meter focal length. A shorter focal length would have created even larger spot sizes, which we have already seen are too large for a useful daytime Raman lidar. And even at this focal length, an auxiliary cylindrical lens would be required to improve the focus quality of the off-axis Raman signals due to the large spots measured. All of these factors indicated that the use of an HOE for a Raman lidar system at this time would make scanning difficult and would not permit daytime measurements. It would be necessary to rotate the cylindrical lens and detectors along with the HOE itself in order to make measurements. This places stringent mechanical requirements on the scanning system in order to maintain the desired resolution. Nonetheless, the HOE was used to make nighttime measurements of atmospheric nitrogen. These tests were published [11] and constitute the first measurements of Raman scattering using an HOE telescope.

So for reasons both of optical performance and mechanical complexity, we determined that the HOE technology was not mature enough for use in a Raman lidar system at this time. Therefore, we decided to investigate theoretically what the performance of a similar power-aperture product Raman lidar would be if we based it on a traditional telescope. Since scanning did not seem to be an option with the HOE approach, the use of a traditional telescope seemed to offer only improvements in all other performance categories compared to the HOE approach. The name that we adopted for the system under investigation was RASL - Raman Airborne Spectroscopic Lidar.

## **5.2 Years 2 and 3**

The second and third year of the activity were spent in determining the optimized configuration of an airborne Raman water vapor lidar based on a traditional telescope and then designing, fabricating and testing the system. Certain

component technologies of RASL such as the data acquisition system, optical filters and receiver module could be tested during the second year while major components of the actual RASL such as the laser and telescope were still being manufactured.

### **5.2.1 Raman Airborne Spectroscopic Lidar**

We desired to develop an airborne Raman lidar optimized for measurements of water vapor mixing ratio, aerosol extinction/optical depth/depolarization and extinction/backscatter ratio during both the daytime and nighttime. We also desired to measure cloud liquid water although these measurements would initially be limited to nighttime only. This broad measurement suite would represent a dramatic increase in airborne remote sensing capability beyond that of any existing airborne lidar. In determining how to size the components of RASL, we considered several research aircraft with which we would like it to be compatible.

The DC-8 is one of NASA's primary research aircraft. The DC-8 cargo bay is an attractive choice for the installation of RASL instrument because it is relatively little used for instrumentation and it possesses a large downward looking viewport. A concept drawing showing RASL installed in the DC-8 is shown in figure 3. This part of the aircraft is limited to approximately 4 feet in height. RASL therefore signifies a large reduction in weight and size compared to traditional ground-based Raman lidar systems. However, the cargo bay can experience considerable temperature fluctuations during flight. Therefore the RASL telescope would have to be designed to be essentially insensitive to temperature fluctuations. But the temperature changes would still be a significant concern for laser operations. In order to maintain stable laser power, we will need to implement a feedback system to stabilize the laser power. We also considered the flight environment of the P-3, C-130, ER-2 and WB-57 and concluded that, in some cases with modifications to enclosure pods (in the case of the ER-2 and WB-57), that a RASL system of the specifications shown in the following table was either compatible with or could be made compatible with all these aircraft.

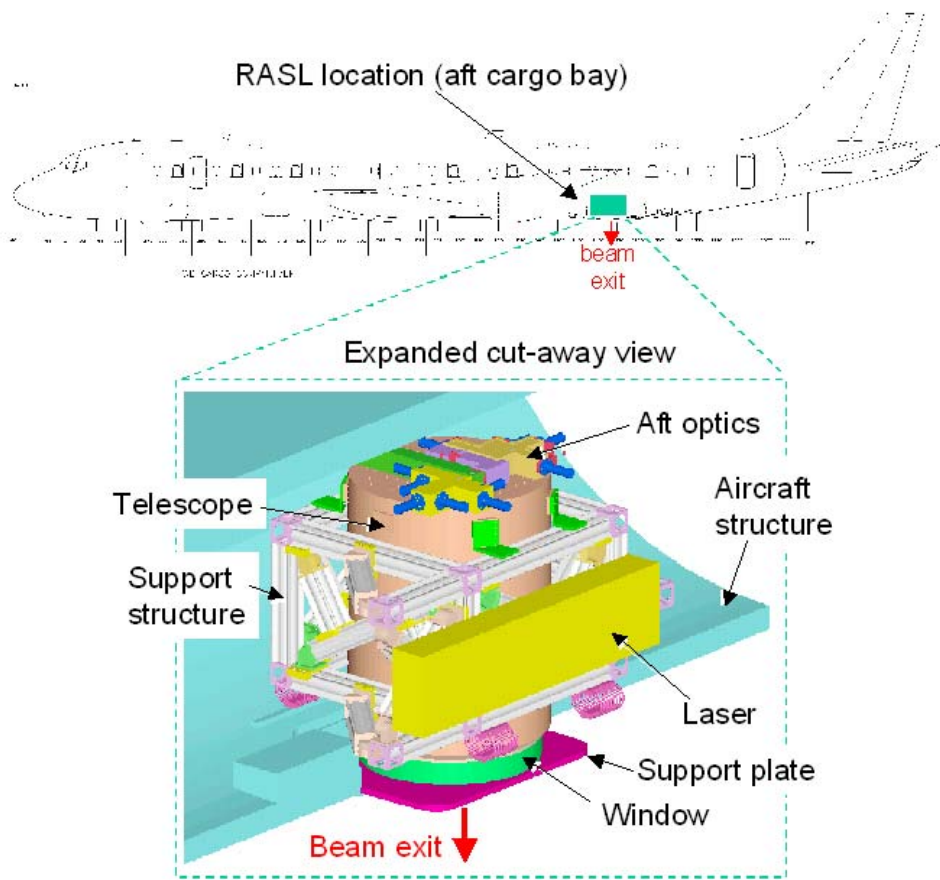


Figure 3: Concept drawing of RASL installed in the NASA DC-8 cargo bay.

<b>RASL Specifications</b>	
Laser	Continuum 9050Nd:YAG (355 nm), 350 mj/pulse, 50 Hz
Telescope	Custom 24" athermal, manufactured by DFM Engineering
Data acquisition	250 Mhz photon counting and 20 Mhz analog detection
Range resolution	7.5 meter
Measurements	
Wavelength (nm)/Bandpass (nm)	
	water vapor/407.5/0.25
	liquid water/403.2/6.0
	nitrogen/386.7/0.3
	oxygen/375/0.3 or CO <sub>2</sub> /371.6/0.3
	elastic unpolarized/354.7/0.3
	elastic parallel polarized/354.7/0.3
	elastic perpendicular polarized/354.7/0.3
Detectors	Hamamatsu R1924 (Raman) and R7400 (aerosol) PMTs
Field of View	0.25 mrad

### 5.2.2 Current airborne water vapor lidars

Current airborne water vapor lidars use the differential absorption lidar (DIAL) technique. This technique makes use of the differential extinction of two closely spaced wavelengths (1 absorbed, the other less so or not at all) to calculate the water vapor density as a function of range. The DIAL technique is used in such systems as the LE-ANDRE (Service D'Aeronomie, Universite Pierre et Marie Curie, Paris, France, <http://www.aero.jussieu.fr/>), the German Aerospace Research Center (DLR, Deutsches Zentrum für Luft- und Raumfahrt, <http://www.op.dlr.de/ipa/LIDAR/Wasserdampf/wasserdampf.htm>) H<sub>2</sub>O DIAL, and the Langley Research Center LASE (Lidar Atmospheric Sensing Experiment, <http://asd-www.larc.nasa.gov/lase/ASDLase.html>). Systems such as these have been quite successful in charting the evolution of water vapor in the atmosphere and have significantly improved our understanding of atmospheric water vapor. To perform these measurements, the lasers used in DIAL experiments must be able to operate on and off of one or more water vapor absorption features and are therefore expensive, custom, narrow line lasers, which require precise control of the outgoing laser spectrum. However, provided that accurate spectroscopy of the water vapor lines is available and that one maintains precise knowledge of the spectral purity of the laser and the exact location of the laser line center for each shot, a DIAL water vapor lidar is self-calibrating. The wavelengths that are currently in use by these laser are typically in the near IR region of the spectrum (815 nm and 940 nm bands) and thus present a significant eye-safety concern. Furthermore, the additional measurements that these DIAL systems can

make simultaneously with that of water vapor are limited.

Recent advances in lasers and electro-optics now permit a daytime and nighttime capable Raman water vapor lidar to be easily deployed in an aircraft. The RASL system will be the first such instrument. By contrast to the DIAL systems mentioned above, it will enable a broad range of useful atmospheric measurements to be performed in addition to that of water vapor using much simpler laser technology while presenting a dramatically reduced eye-safety hazard. The following table summarizes some of the key distinctions between a typical DIAL water vapor lidar and RASL. In this comparison, the power of the Raman technique, which takes advantage of the natural spectroscopy that occurs in the atmosphere due to a single exciting wavelength, is clear.

	Water Vapor DIAL	RASL
Laser	custom, tunable, high spectral purity	Off the shelf
Measurements		
water vapor	yes	yes
cirrus cloud optical depth	yes, in the absence of volcanic aerosols	yes
cirrus multiple scattering	no	yes
cirrus cloud equivalent particle radius	no	yes
cirrus ice water content	no	current research topic
aerosol scattering ratio	yes if use molecular density profile	yes
aerosol extinction	yes if use assumed $S_a$ profile	yes
aerosol optical depth	yes if use assumed $S_a$ profile	yes
aerosol extinction/backscatter ratio ( $S_a$ )	no	yes
aerosol depolarization	yes (possible but typically not done)	yes
cloud liquid water (LW)	no	yes, concept demonstrated[16]
cloud droplet radius	no	yes, concept demonstrated[16]
cloud droplet number density	no	yes, concept demonstrated[16]
Eye Safe Distance	~8 km	~0.5 km
Cost	~\$5-\$10m	\$2m (estimate for fully flight ready system)
<i>Comparison of a typical water vapor DIAL lidar and RASL</i>		

### 5.2.3 Comparison of LASE water vapor measurements and RASL simulation

A strong verification of the design parameters for RASL was provided through numerical simulation [19] of the system and comparison of these measurement capabilities with those of existing water vapor sensors. A sophisticated numerical model was constructed and first used to match actual ground based data acquired by two Raman lidar

systems. After this ground based validation of the model, it was then used to predict the performance of RASL under a wide range of conditions. In figure 4 is shown both nighttime and daytime simulations of the RASL airborne lidar under sub-tropical conditions with the assumption that the daytime measurements are over an ocean surface with 10 degree solar zenith angle.

The nighttime simulations of RASL used a 10 second integration time while the integration time used for the daytime simulations was 3 minutes. The random error of the RASL measurements is 5% or less at the surface for both simulations. A three minute integration of the Langley Research Center Laser Atmospheric Sensing Experiment (LASE) differential absorption water vapor lidar measurements acquired at nearly the same time as the nighttime radiosonde are shown for comparison. The vertical resolution of the plotted data is as follows: LASE: 0-2 km: 330m, 2-6 km: 510m, 6-8 km: 990m, RASL (night) 0-4 km: 150m, 4-7 km: 90m, 7-9 km: 40m, RASL (day) 0-4 km: 300m, 4-7 km: 150m, 7-9 km: 40m. (The disagreement between LASE and the sonde between ~1-2 km is likely due to atmospheric variation and not instrument performance). These simulations indicate that, under these conditions, a Raman lidar of the current specifications of the RASL system has considerably higher temporal (approximately a factor of 20) and spatial resolution (varies between a factor of 2 and a factor of 20) during the nighttime than the LASE instrument and comparable temporal but still improved spatial resolution during the daytime. These measurements are possible with RASL while maintaining a significantly lower eye-safety hazard.

As discussed in [19], there are several important advantages that permit a Raman lidar system operating from the air to produce improved measurements versus the same system operating from the ground. Those advantages include the dynamic range compression that results by looking downward versus upward. This allows the full range of the signal from a 10 km flight altitude to be measured with a single detector as opposed to the two channels required for ground based operations. Also, the background sky light is typically lower looking downward compared to looking upward. This results in improved daytime performance for downward-looking airborne operations.

The other advantage of RASL is the inclusion of numerous other high priority ESE measurements in addition to water vapor. The simultaneous measurement of water vapor mixing ratio, cloud liquid water, aerosol scattering ratio, aerosol extinction, aerosol optical depth and aerosol depolarization will permit a range of atmospheric studies not

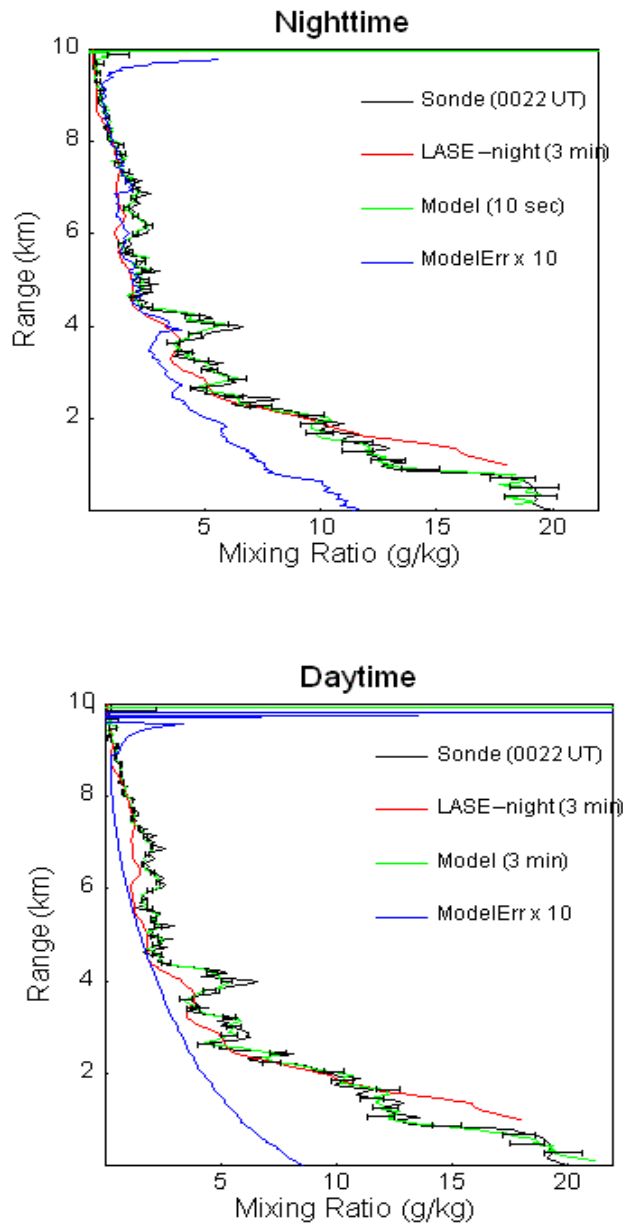


Figure 4: Comparison of simulated RASL, sonde and LASE measurements. The current RASL optical configuration and a radiosonde measurement of water vapor were used as input to the model. On the top is the comparison of simulated nighttime RASL measurements with the other sensors where the RASL integration time was 10 seconds. On the bottom is the corresponding daytime comparison using 3 minutes of integration for the RASL measurements. The same LASE measurements (acquired at night using 3 minutes of integration) and sonde data are shown in both plots. In the nighttime simulation, the integration time for RASL is approximately a factor of 20 less than for LASE while still preserving higher vertical resolution. See text for further details.

possible with any current airborne lidar system. From the proper flight altitude or by looking upward, cirrus extinction and optical depth are also possible. Furthermore, the quantification of cirrus particle size has been demonstrated [20] based on the multiple scattering in cirrus clouds. With some assumptions, this measurement of particle radius can be converted into an estimation of ice water content. Therefore RASL will potentially be capable of quantifying all three phases of water. Measurements such as these are crucial to an understanding of the water cycle and radiative transfer in the atmosphere.

#### **5.2.4 System Design**

The preceding considerations of compatibility with existing aircraft and performance with respect to existing sensors established the design criteria for the actual RASL hardware. The major system components that required custom design to meet our requirements were the telescope and the optical detection package since the required laser was available as an off-the-shelf system. Although this IIP was funded just for laboratory demonstration of the main RASL components leaving system frame, aircraft integration and flight time to a future proposal, we nonetheless also investigated the requirements for the instrument frame and aircraft window that would be required by RASL for full airborne testing.

##### **Telescope**

The telescope design constraints were determined in-house. A diagram of the telescope mounted in an aircraft was generated to help inform the bidders of the intended use of the telescope. That is shown in figure 5.

The successful bidder was DFM Engineering of Longmont, Colorado. The resulting design parameters are shown in the following table. The most conspicuous features of the system are its athermal design and its compact structure given the 0.6 m aperture.

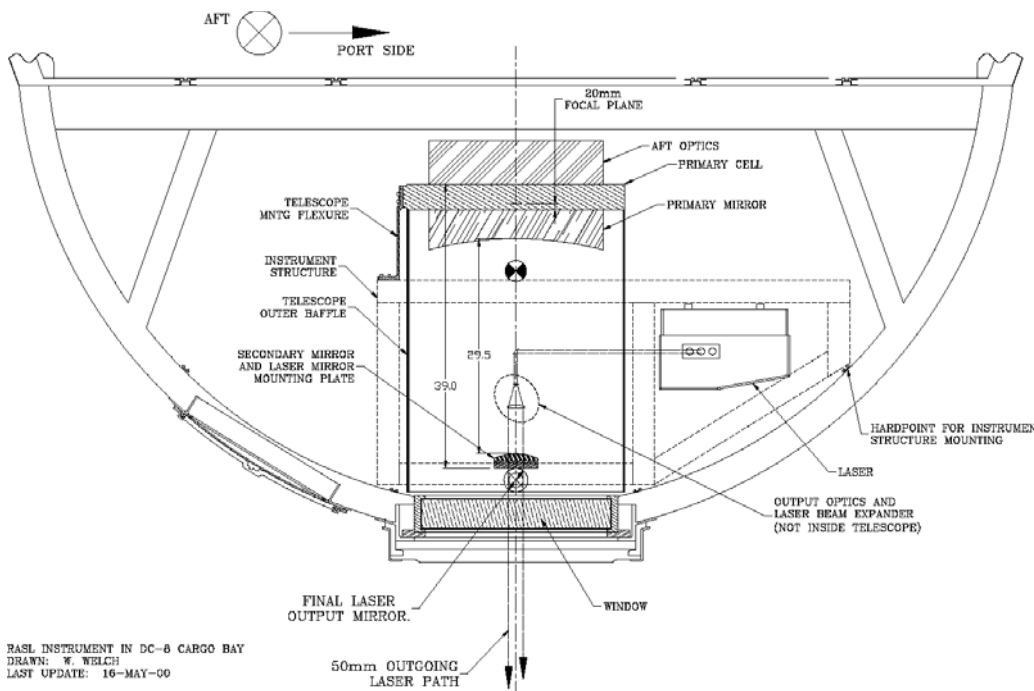


Figure 5: Diagram of the RASL telescope mounted in the cargo bay of the DC-8. This diagram was sent along with the statement of work for bids on the RASL telescope.

## System Level Specifications

Aperture Diameter	24.0" (608.6mm)
Effective Focal Length:	126.96" (3224.8mm) +/-5%
Telescope System f/#:	f/5.3
Back Focal Distance	8.29" (210.5mm) past primary mirror vertex
Flange Focal Distance:	0.787" (20.0mm) past aft-optics mounting plate
Image Quality (On-axis):	blur circle < 25urad diameter @ 90% encircled energy
Field of View:	adjustable, 0.20mrad to 2.00mrad

Mirror Specifications	Primary (M1):	Secondary (M2)
Diameter (clear aperture)	24.0" (609.6mm)	7.5" (190.5mm)
Center Thickness	~4.0" (101.6mm) at 6:1	~1.0" (25.4mm) at 8:1
Radius of Curvature	-84.0" (2133.6mm) concave	-37.359" convex
Conic Constant	-0.650195 (ellipse)	0.000 (sphere)
Inter-vertex Separation:	29.5" (749.3mm)	
Mirror Substrates:	Zerodur or other instrument quality substrate material.	
Primary Mirror f/#	Nominal is f/1.75, we are also interested in pricing for an f/1.50 primary	
Mirror Coatings:	Option #1: Rmax (>99% Goal) from 350nm to 410nm Option #2: R > 95% from 350-410nm and 530nm-680nm	

*Design parameters for RASL telescope*

## Optical detection system

RASL measurement requirements dictated that the optical detection system measure signals at resolutions ranging from ~1 Angstrom to 6 nm spanning a spectral range from 355 nm to 410 nm. Longer wavelengths can be included in the future through fiber coupling. The desired optical detection channels are listed in table below.

Measurement	Wavelength (nm)	Bandpass (nm)	Detector
Rayleigh-Mie unpolarized AD	354.7	0.3	Hamamatsu 1924 or 7400
Rayleigh-Mie unpolarized PC/AD	354.7	0.3	Hamamatsu 1924 or 7400
Rayleigh-Mie parallel polarized AD	354.7	0.3	Hamamatsu 1924 or 7400
Rayleigh-Mie parallel polarized PC/AD	354.7	0.3	Hamamatsu 1924 or 7400
Rayleigh-Mie perpendicular polarized AD	354.7	0.3	Hamamatsu 1924 or 7400
Rayleigh-Mie perpendicular polarized PC/AD	354.7	0.3	Hamamatsu 1924 or 7400
Bore-site alignment	354.7	0.3	Hamamatsu 7546 multi-anode
Raman oxygen or CO <sub>2</sub>	375 or 372	0.3	Hamamatsu 1924
Raman nitrogen	386.6	0.3	Hamamatsu 1924
Raman liquid water	403	6.5	Hamamatsu 1924
Raman water vapor	407.5	0.25	Hamamatsu 1924

*Description of 11 RASL channels including wavelengths, bandpasses and detectors*

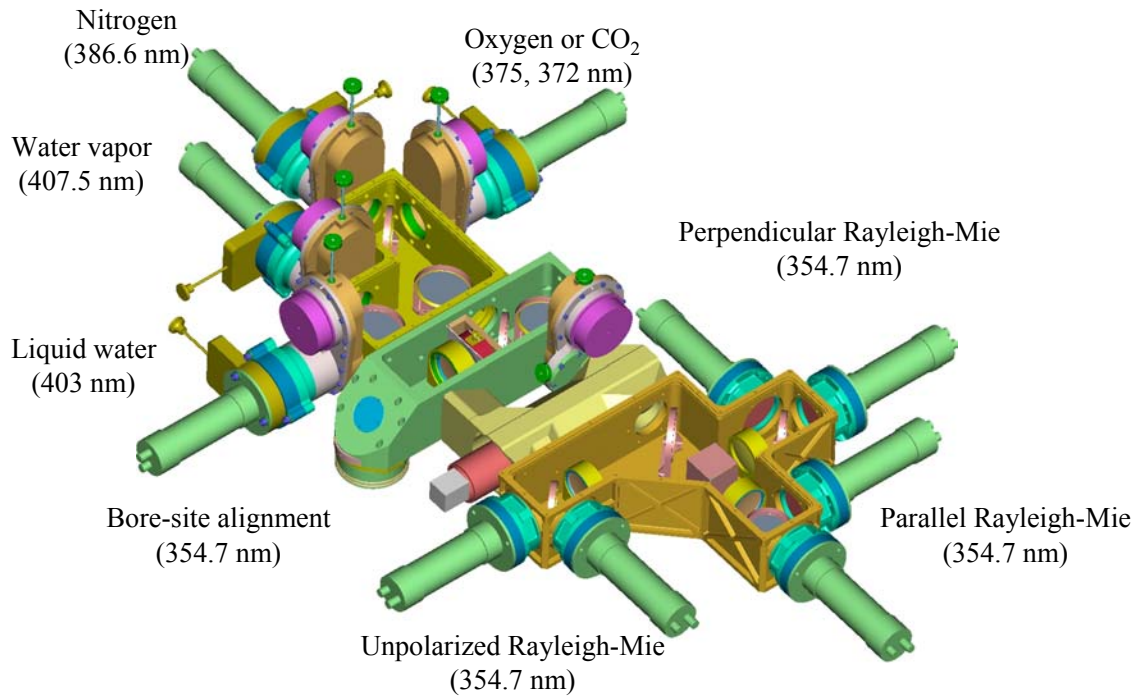


Figure 6: Schematic layout of the RASL optical detection system.

A concept layout of the optical detection package is shown in figure 6. Photographs of the RASL telescope with the optics packaged installed is shown in figure 7.

### **Laser**

A survey of the commercially available lasers was performed and a statement of work was generated consistent with both the measurement requirements of RASL as well as feasibility based on the survey. Proposals were received from two vendors: Continuum and Spectron Lasers. However only the proposal submitted by Continuum, Inc. of Santa Clara, CA fully met the requirements laid out in the RFP. Therefore, a Continuum 9050 laser was procured for use in the RASL system. A diagram of the layout of the laser head is shown in figure 8. A photograph of the laser installed in the Raman lidar lab is shown in figure 9.

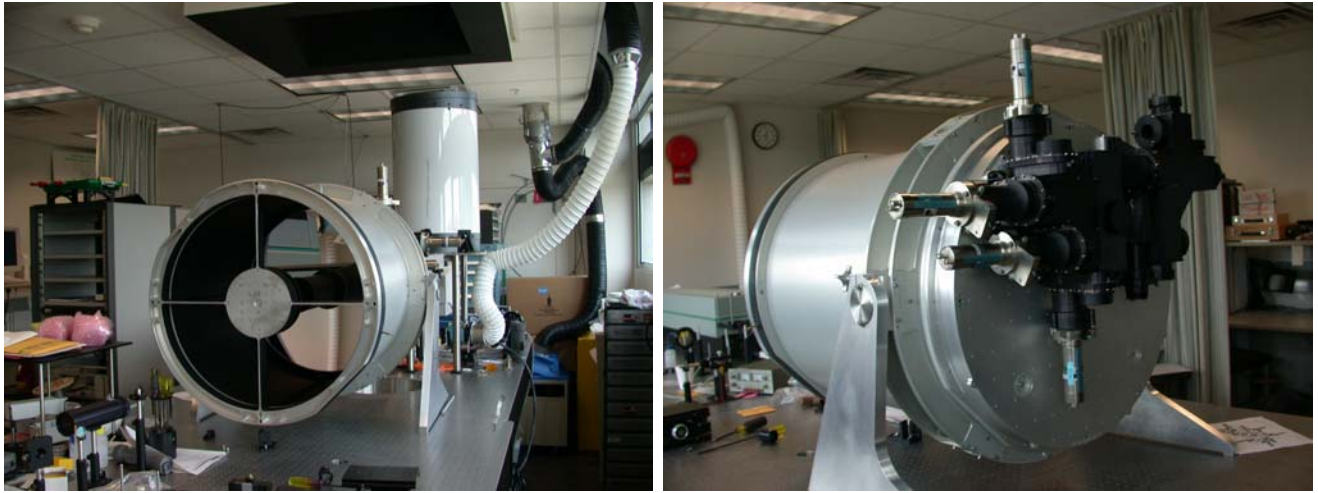


Figure 7: The RASL telescope during installation of the optical detection package on the backplate of the primary. Not all of the photomultiplier detectors were installed at the time of this photograph.

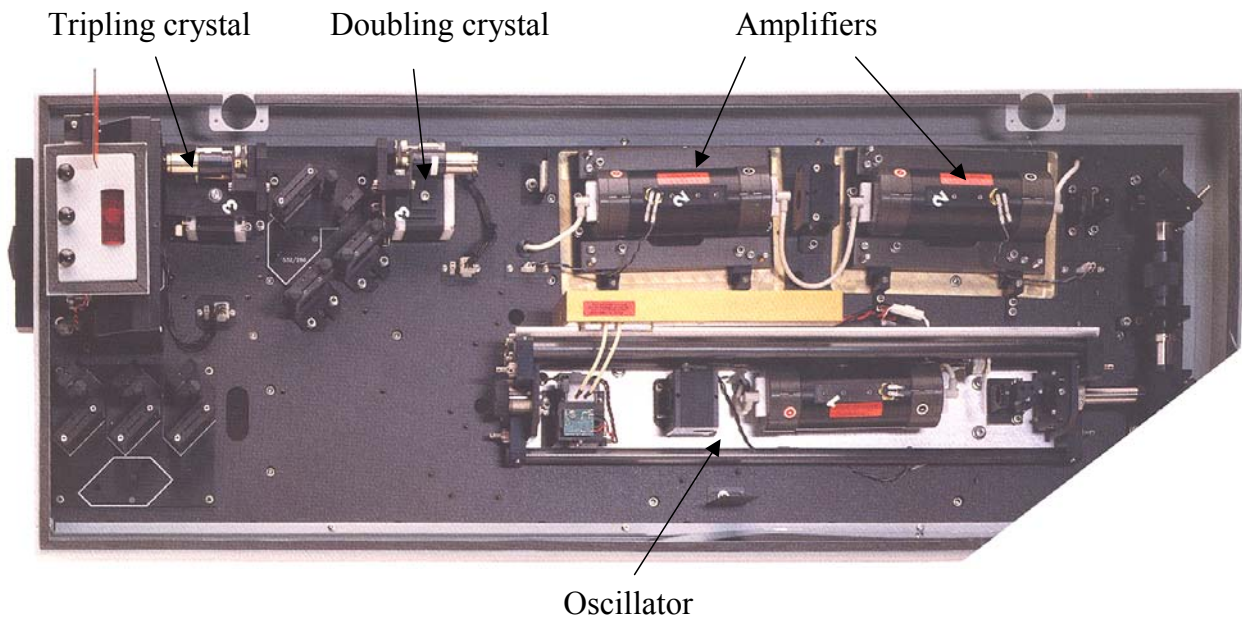


Figure 8: Continuum 9050 laser head.



Figure 9: The Continuum 9050 laser (with cover open) is shown in the Raman lidar lab. The RASL telescope is pointed upward through the roof hatch in order to acquire the test measurements shown in this report.

### **Data acquisition system**

The desire to create a daytime/nighttime water vapor Raman lidar demanded that the data acquisition system be able to handle very high photon count rates. Photon counting systems are subject to nonlinearities at high count rates due to the large increase in the probability that two photons will arrive spaced closely enough in time so as to be indistinguishable from a single pulse. Various correction techniques have been applied to this type of data in the past with varying degrees of success. To circumvent the need to correct for photon counting nonlinearities, data acquisition devices from Licel Corporation of Berlin Germany were selected for the RASL instrument. These devices record the input waveform simultaneously with photon counting (250 Mhz bandwidth) and 12-bit analog to digital (20 Mhz bandwidth) electronics. The signals are combined in post processing in such a way as to avoid high photon count rates; above a certain count rate where the photon counting is still linear, the analog signal is used. The data acquisition system with Licel transient recorders controlled by a PC running LabView is shown in figure 10.

### **Aircraft window**

The current IIP effort was to design, build and demonstrate in the laboratory the components of an optimized airborne Raman lidar. Mechanical components required for actual flight of the instrument such as the frame and a UV grade transmission window as well as electronic feedback systems to maintain laser power and bore-site alignment were not funded under this IIP. However, both the instrument frame and the aircraft window were viewed as such a critical elements that research was done into the feasibility and cost of these required components. The testing and environmental requirements for the window were obtained from Dryden Research Center. Designs were generated which met their specifications and vendors were then contacted to obtain price and delivery. Two approaches were identified for design and construction of the window. The first was a solid fused silica window anti-reflection coated for the desired RASL wavelengths with the center hard-coated for laser transmission. Alternate designs included a matrix structure of smaller windows that were held within a frame assembly. The estimate for a solid fused silica window with coating was \$75k. It was found that >80% of the useful aperture could be maintained in the RASL window using the matrix approach while decreasing the cost of the window ~40%. A schematic of fully assembled RASL installed in the P-3



Figure 10: RASL data acquisition system (6 channels shown) with combined photon counting and analog detection electronics from Licel Corp of Berlin, Germany. The system is driven by a PC running LabView.

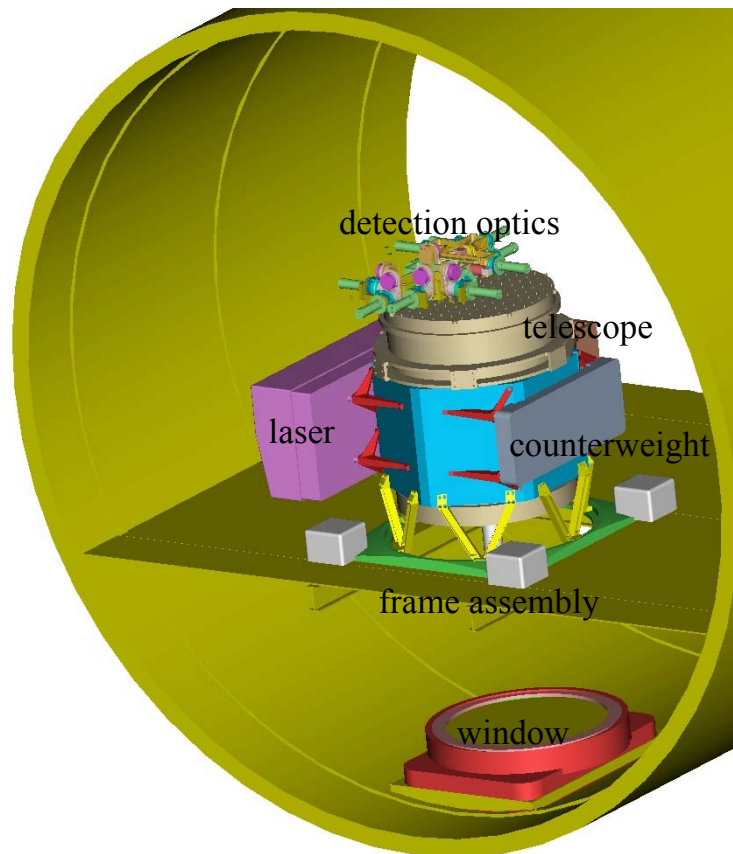


Figure 11: Example installation of the RASL instrument in the P-3 aircraft. The aircraft window is at the bottom of the cargo bay while the RASL instrument itself is mounted in the passenger compartment.

aircraft is shown in figure 11. The window is at the bottom of the aircraft cargo bay while the instrument is installed in the passenger compartment. The conceptual design of the RASL frame is also shown.

### 5.2.5 Validation of RASL technologies during IHOP

Certain crucial RASL technologies were validated through their use in field deployments of the Scanning Raman Lidar (SRL). The SRL participated in the International H<sub>2</sub>O Project held in western Oklahoma in May - June, 2002. The RASL data acquisition systems and optical filters were tested during this deployment. The addition of these components to the SRL enabled the system to demonstrate the highest signal to noise Raman lidar measurements of water vapor mixing ratio ever made during the daytime. Some of these measurements are shown in figure 12.

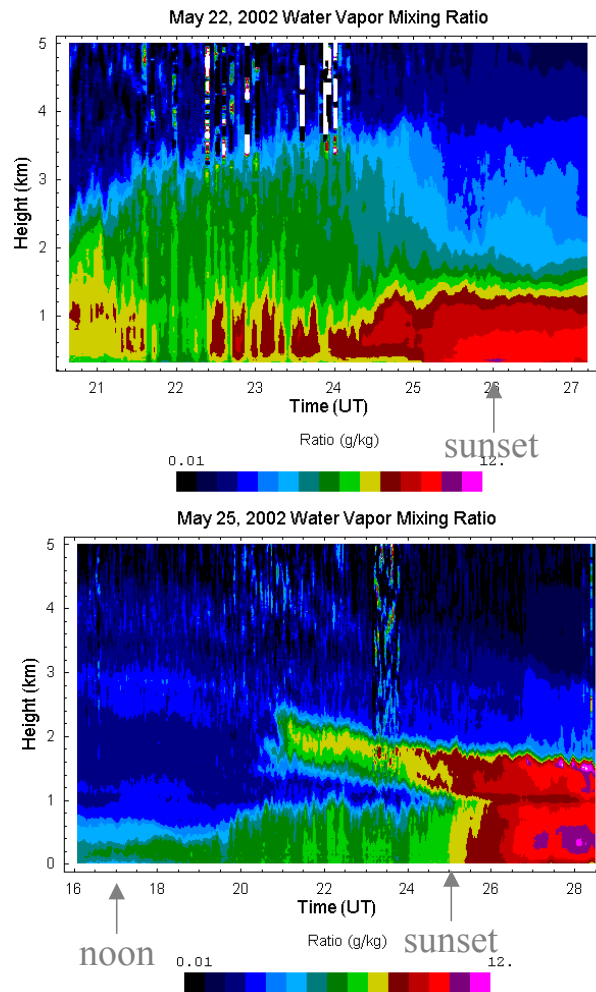


Figure 12: Measurements of water vapor mixing ratio taken during during the IHOP field campaign under day and night conditions by the NASA/GSFC Scanning Raman Lidar using RASL optical filters and data acquisition electronics.

The image at the top of the figure shows the water vapor evolution during a dryline event near the SRL location. The growth of the boundary layer caused by solar heating during the daytime is seen as the day progressed until 2400 UT when the dryline moved closest to the lidar location creating a moistening effect in the lowest layers and a distinct drying above. The image at the bottom of the figure shows the mixing of two distinct water vapor air masses. These measurements used 3 minute temporal and between 200 and 400 meter spatial resolution. Measurements of water vapor with such high resolution will permit dynamical studies of storm initiation mechanisms that were not previously possible. These measurements also provided strong validation of the approach being pursued for RASL and confirmed the assumptions of the numerical modeling [19] used to help establish the design parameters of RASL.

#### **5.2.6 Final assembly and test - first RASL measurements**

The delivery of all optical components of RASL was completed in June, 2002. Acceptance testing was done to verify that they met specification. At this point assembly and alignment of the telescope/optics package began. The first major task to be accomplished was the verification of the focus position of the RASL telescope. The focus position was verified using two approaches: using an external collimated beam and performing a retroreflection test using the RASL telescope itself. After determining this position, the RASL aft optics were installed. The optical channels were aligned by illuminating the field stop which was set at it's minimum field of view. All channels were aligned using this approach.

Atmospheric testing of the final RASL optical configuration began in September, 2002. The first atmospheric measurements were taken during a data acquisition period of more than 24 continuous hours on September 17-18. Although the laser was operating at only half power due to the need to change the flashlamps and that other system parameters had not been optimized, the performance of the system when first used was sufficient to demonstrate all the major atmospheric measurements designed into the RASL system: water vapor mixing ratio, aerosol backscatter/extinction/depolarization, liquid water mixing ratio, cirrus cloud optical depth and extinction to backscatter ratio. The first measurements ever made with the RASL will now be presented. Although the processing is only preliminary, these measurements demonstrate that the RASL system meets all measurement requirements established for the sys-

tem and, once airborne, will offer a dramatic improvement in atmospheric measurement capability over any existing airborne lidar system.

### **Water vapor mixing ratio**

The NASA/GSFC Raman lidar group is funded to support the Aqua satellite through ground-based measurements of water vapor and cirrus clouds. The first measurements of RASL were acquired during a period that coincided with an Aqua overpass validation exercise on the morning of September 18, 2002. At 3:01 am EDT, the Aqua satellite was at its peak elevation angle of 77.5 degrees with respect to NASA/GSFC. The Raman lidar group launches radiosondes and measures atmospheric water vapor using their Scanning Raman Lidar (SRL) instrument during these overpasses. The first measurements of RASL encompassed these validation exercises affording the opportunity to compare RASL with SRL and radiosonde measurements of water vapor. A comparison of those measurements is shown in figure 13 where the lidar measurements have been calibrated based on a precipitable water comparison with respect to a SuomiNet GPS measurement of total precipitable water (The Raman lidar group is a participant in the SuomiNet network of GPS systems. We maintain two such systems: one permanently installed at NASA/GSFC and another that is installed on our mobile Scanning Raman Lidar and used for field calibration of the lidar. Information on SuomiNet can be found at <http://www.unidata.ucar.edu/suominet/>). The figure shows very good agreement between the two Raman lidar measurements of water vapor mixing ratio (g/kg) as should be expected for two properly functioning systems. Above ~2km there is a consistent wet-bias seen in the radiosonde data with respect to the lidar measurements. This could be due to real atmospheric variations between the lidars, which measure purely vertical profiles, and the radiosonde, which drifts with the wind and may intercept different atmospheric conditions. There could also be differences due to either radiosonde or lidar sensor inaccuracies, however past comparisons have shown excellent agreements between Raman lidar and a host of other sensors while the Sippican radiosonde package has shown considerable variability in its water vapor measurements. Because of the generally good agreement of the two lidar systems, it is believed that the radiosonde measurements are biased wet above ~2km on this night although other measurements would be required to establish this with certainty.

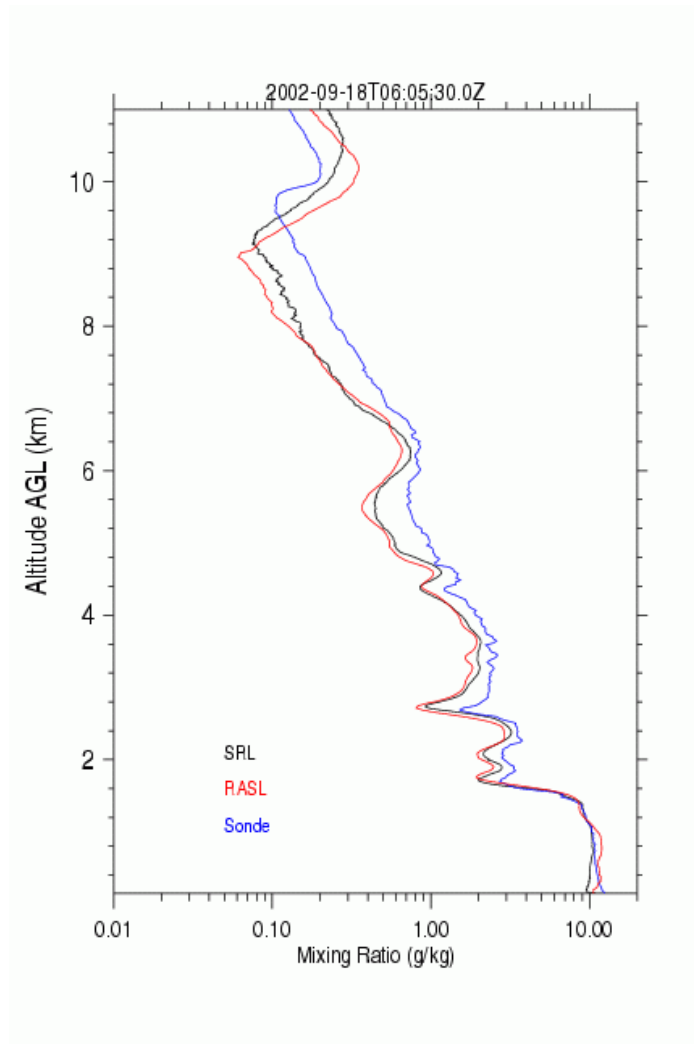


Figure 13: Comparison of the water vapor mixing ratio profile of RASL, the NASA/GSFC Scanning Raman lidar and radiosonde launched at GSFC on the night of September 18, 2002. These measurements were made during the overpass of the Aqua satellite and will be used as part of the validation campaign for Aqua.

Color images of the time series of water vapor, one during the nighttime the other during the daytime, are shown in figure 14. On the top is shown the nighttime image of water vapor mixing ratio while the daytime image is on the bottom. The increased turbulence in the daytime image due to solar heating is clear. Small processing glitches caused either by a realignment of the lidar system or by an incorrect detection of the laser fire in the data (and that will be removed once the data are processed fully) can be seen at, for example, 2200 local in the nighttime image and at 1600 in the daytime image. These measurements more than confirm the predictions of RASL measurement quality based on numerical modeling studies [19]. Those studies indicated that an airborne Raman lidar of the configuration of RASL would offer high quality water vapor profiles in as little as 15 seconds; a dramatic decrease in the averaging time required for such profiles compared with existing airborne lidars.

#### **Aerosol scattering ratio, aerosol depolarization, cirrus cloud optical depth and extinction/backscatter ratio**

Cirrus clouds strongly affect the earth's radiation balance and when optically thin are difficult to detect by satellite. A Raman lidar system with the capabilities of RASL is highly sensitive to the presence of cirrus clouds and can be used to detect their presence and quantify their optical depth even for clouds below the detection threshold for satellites [20]. This is the focus of the Raman lidar group's participation in Aqua validation: to study the influence of thin cirrus clouds on water vapor retrievals of the Aqua water vapor sensors.

Cirrus clouds were present during most of the 24-hour measurement period of RASL. The scattering ratio of the cirrus clouds (where a scattering ratio of 1 defines pure molecular scattering and a ratio of 2 implies that the cirrus scattering is equal to the molecular scattering at the same altitude) is shown in figure 15. The nighttime image is shown on the top and the daytime image is shown on the bottom. During the period the cirrus clouds descended in altitude. Periods of cirrus precipitation (fall streaks) are visible in the nighttime image at 1500 UT. The scattering due to boundary layer aerosols is also visible in the lower 1.5 km. The vertical stripes in the data above the cirrus clouds at certain times such as 0100 local indicate noise due to attenuation of the laser beam. Notice that the geometrical thickness of the clouds is generally much lower during the daytime period.

The daytime depolarization data corresponding to the bottom image in figure 15 can be used to study the different

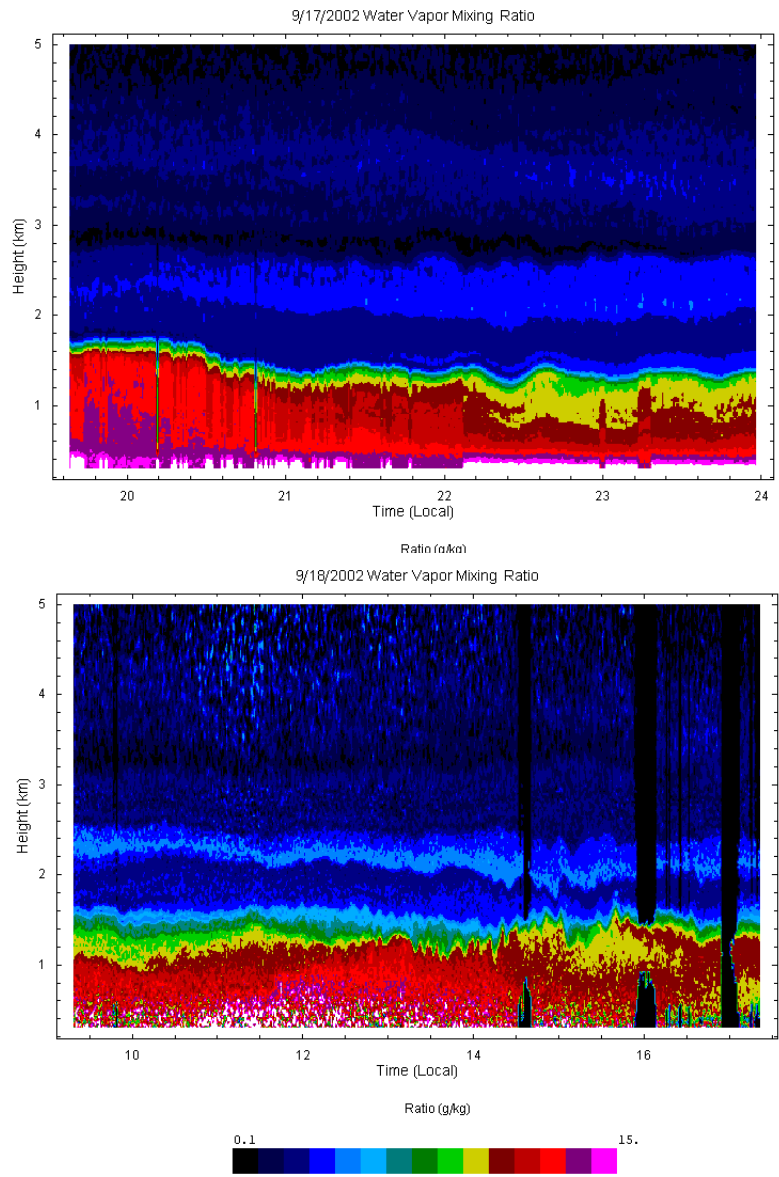


Figure 14: Nighttime (above) and daytime (below) images of water vapor mixing ratio acquired during the first data acquisition session of the RASL instrument.

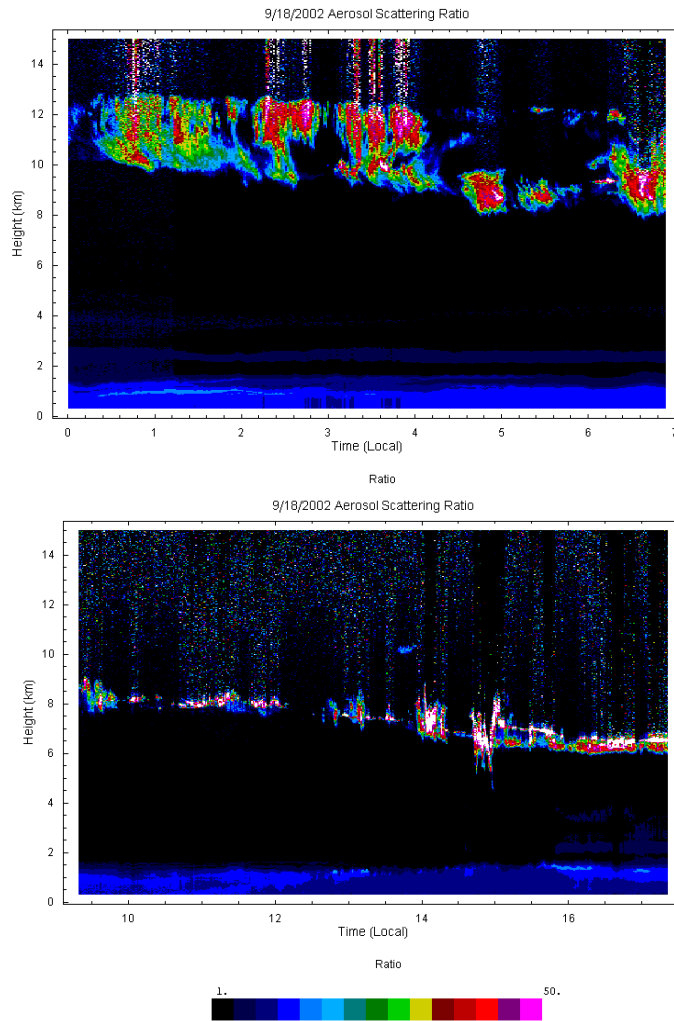


Figure 15: Aerosol scattering ratio measurements during nighttime (top) and daytime (bottom) of cirrus clouds as they evolved over building 33 at NASA/GSFC. Notice the lowering of the layer as time progressed.

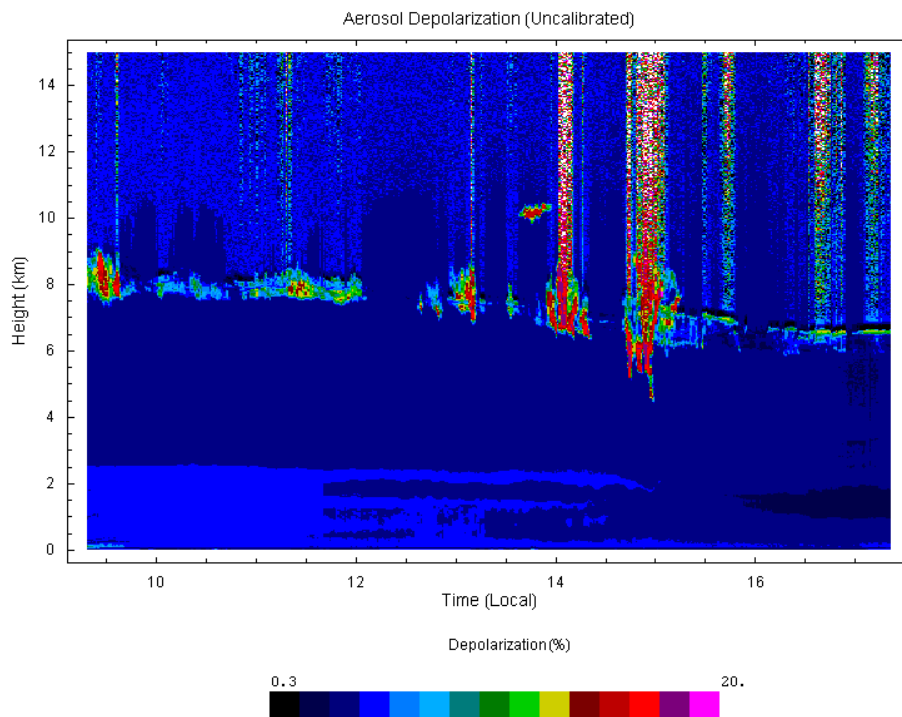


Figure 16: The corresponding depolarization image for the daytime cirrus measurements shown above. Precipitation of ice crystals as well as regions of mixed phase (ice and water together) can be discerned in this image.

clouds types and dynamical processes that occurred during the daytime part of this measurement period. These data are shown in figure 16. Frozen precipitation (fall streaks) are present at 1500 local and at an altitude of ~6 km. The precipitating cirrus particles can be expected to be large and therefore highly depolarizing as shown in the image. By contrast, the thin clouds that follow this precipitation event show very low depolarization at the tops as indicated by the black color. This indicates a mixed phase cloud where the upper part of the cloud is super-cooled liquid water. Crystallization causes ice particles to grow and descend so that the depolarization is higher in the lower portions of the cloud. This is an example of how RASL measurements can be used to discern physical and dynamical processes in cirrus clouds.

The Raman lidar can also be used to quantify in a direct way the cirrus cloud optical depth and the mean extinction to backscatter ratio. These are quantities that are difficult or impossible to determine with an elastic lidar system.

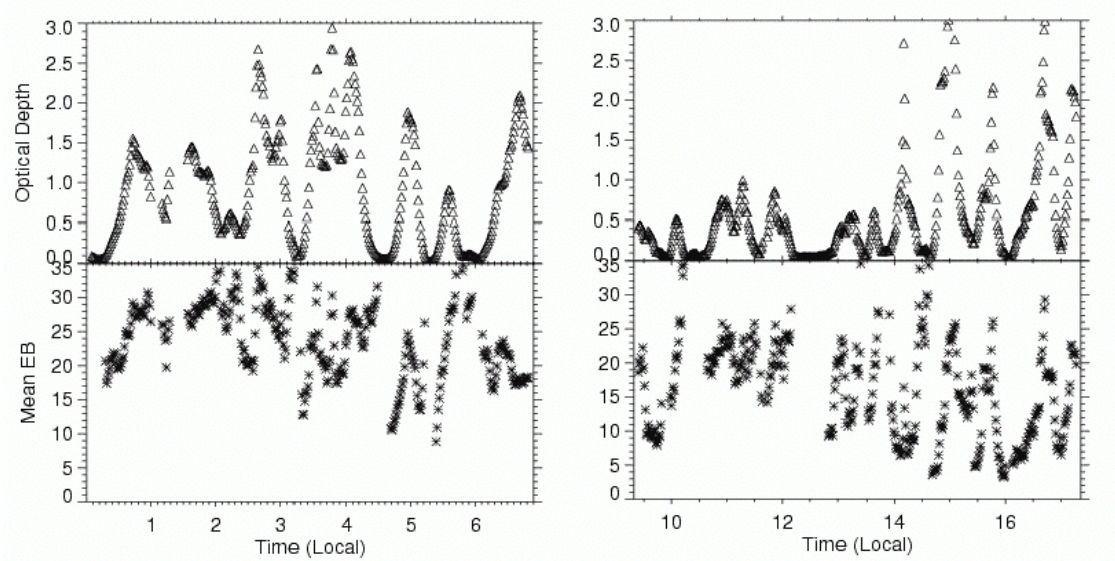


Figure 17: Cloud optical depth and extinction to backscatter ratio as measured by the RASL instrument. On the left is shown the nighttime retrievals during the presence of cirrus clouds. On the right are daytime retrievals during mixed phase clouds. The mean extinction to backscatter ratio for the cirrus clouds is  $\sim 24$  while for the mixed phase clouds it is  $\sim 18$ .

Furthermore, under conditions of tropospheric aerosol loading the extinction to backscatter values for different cloud types are needed by elastic only lidar systems such as the upcoming lidar systems on GLAS and CALIPSO in order to estimate cloud optical depth. As shown in figure 17, RASL can directly quantify these cloud parameters offering great potential for validation of these upcoming space-based lidar systems.

On the left of figure 17 are shown the optical depth and the mean extinction to backscatter (EB) retrievals during the nighttime measurements of cirrus clouds shown in figure 15. The average value of EB for these nighttime cirrus clouds was  $\sim 24$ . On the right is shown the same data products for the mixed phase clouds shown in the daytime. The optical depths were in general lower for these clouds. Also the average EB was  $\sim 18$ . Knowledge of the variation in the EB values for different cloud types is needed for accurate estimates of cloud optical depths from elastic only lidar data under conditions of tropospheric aerosol loading.

### **Liquid water measurements**

One of the unique measurements of the RASL instrument, a measurement that the NASA/GSFC Raman lidar group is pioneering [13] [16] [17], is that of scattering due to atmospheric liquid water. The original goal of these measurements was to quantify cloud liquid water and permit the retrieval of droplet radius and number density of cloud droplets. That technique has been adopted by other groups in the world [15] and offers a direct measurement of these radiatively important cloud properties in portions of the cloud where competing techniques based on radar have large errors or do not function at all. These capabilities are built into RASL but there were no liquid water clouds present during the measurements of September 17-18.

However, recent research indicates that this technique may also offer an unusually sensitive measurement of liquid water in hydrated aerosols. An example of such measurements is shown in figure 18 where the uncalibrated liquid water mixing ratio (top) is shown along with the estimated aerosol depolarization ratio in the boundary layer. The correspondence of the layers in the liquid water and depolarization images is clear. Much work must be done to validate this new technique but it offers the potential to quantify small amounts of liquid water that have been absorbed by swelling aerosols during the process of growing to become cloud droplets. No other technique exists to remotely quantify this fundamental process in cloud physics.

## **6 Applications of RASL to other science questions**

The utility of the RASL instrument can be further demonstrated by considering the variety of additional measurements that are possible from an airborne platform and how those measurements can be used to address ESE science questions. The quality and utility of the anticipated water vapor measurements from RASL have already been discussed. In addition to these measurements, we expect RASL to be useful for various aerosol measurements and potentially as well to quantify variations in boundary layer CO<sub>2</sub> with sufficient precision to detect correlated changes in CO<sub>2</sub> and H<sub>2</sub>O concentrations.

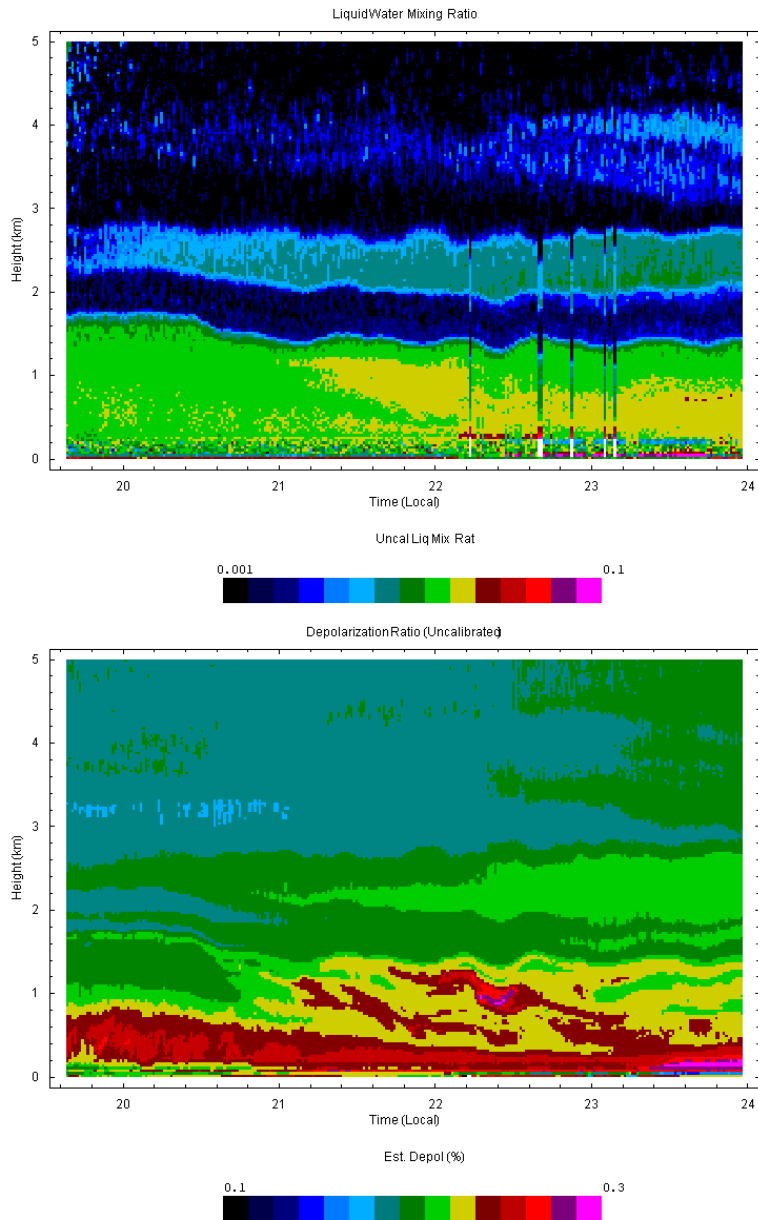


Figure 18: Liquid water (top) and aerosol depolarization (bottom) measurements acquired by RASL during the nighttime. Note the strong correspondence of liquid water and aerosol features. Some scattering enhancement mechanism is at work that permits small amounts of liquid water to be sensed in atmospheric aerosols. (The vertical stripes in the liquid water data are due to an incorrect detection of the time of the laser fire. These errors will be removed in the full processing of the data.)

## **6.1 Aerosol backscatter, extinction, depolarization measurements - TOMS**

One of the great advantages of a Raman lidar is the ability to measure molecular scattering directly. This permits a quantification of aerosol extinction, optical depth and the aerosol extinction to backscatter ratio in the boundary layer. These quantities as well as aerosol depolarization, which can provide information about particle size and phase, will be routinely made by RASL using the 355 nm output of the tripled Nd:YAG laser. These aerosol measurements can be of great use in validation and improvement of tropospheric aerosol retrieval from UV sensors such as the Total Ozone Mapping Spectrometer (TOMS). For example, the current aerosol retrievals from TOMS data do not include information about the height distribution of aerosols. Improvements to these retrievals are in process that will include statistical information about aerosol height from the GOCART aerosol transport model [12], but this still leaves actual aerosol distribution as a distinct error source in the retrievals. RASL measurements of the profile of extinction and extinction/backscatter ratio in the UV would be of great use in validation studies for improving these retrievals. It was not possible to retrieve aerosol extinction in the boundary layer in the measurements presented earlier due to the influence of the overlap function of RASL. However, for an airborne RASL measurements of aerosol extinction and backscatter will be possible in the boundary layer when RASL is flying at nominal altitudes of 5 km or higher.

## **6.2 Fiber optics port - aerosol backscattering and extinction for GLAS and CALIPSO**

All the RASL measurements discussed thus far make use of the tripled Nd:YAG wavelength of 354.7 nm. These measurements include aerosol extinction and backscattering and thus extinction/backscatter ratio. Upcoming laser-based sensors such as GLAS or CALIPSO will calculate aerosol extinction and optical depth using assumptions about the extinction to backscatter ratio ( $S_a$ ) of the aerosols.  $S_a$  is well known to vary widely depending on the actual nature of the aerosols so that uncertainty in this parameters represents a potentially large error source for aerosol measurements by space-borne lidar.

For validation of aerosol extinction and optical depth retrievals by these upcoming instruments, it is possible to scale the 355 nm based measurements of RASL to 532 nm, but this requires assumptions about the aerosol properties. It is much more attractive to emit the 532 nm radiation from the Nd:YAG laser of RASL and to use the fiber optic

port to measure backscattering and extinction using this wavelength. A fiber optic port has been designed into RASL enabling these measurements. The 532 nm radiation emitted by RASL to make these measurements would not be eye-safe at the ground, however. So these measurements are viewed as RASL capabilities which are available for specific validation experiments over unpopulated areas.

### **6.3 CO<sub>2</sub> measurements**

The power of the Raman technique is that a single wavelength is emitted from the laser but a broad range of return wavelengths is available depending on the chemical composition of the atmosphere/target that is being probed. It will be easy to replace the oxygen filter with one designed to measure atmospheric CO<sub>2</sub>. The most attractive CO<sub>2</sub> feature is the  $2\nu_2$  band at a shift of 1285 cm<sup>-1</sup>. Our modeling indicates that the RASL instrument should be able to measure changes in CO<sub>2</sub> concentrations of between 0.6 and 2 ppm from 2.5 km to the surface using a 15 minute integration time (a flight track of ~120 km on the P-3) as shown in figure 19. These measurements would be made simultaneously with (and in the same atmospheric volume as) the water vapor mixing ratio. This would permit studies of the correlation of CO<sub>2</sub> and water vapor concentrations over areas of differing vegetation types to be performed. By flying in a box pattern flux studies could be done downwind of a CO<sub>2</sub> source region or such measurements could be useful for validation of satellite retrievals (e.g. AIRS) of CO<sub>2</sub> in the troposphere where the sensitivity of passive sensors is low. This precision should also be sufficient for studying the variation in CO<sub>2</sub> concentration due to sources and sinks around large bodies of water such as the Great Lakes.

## **7 The future for RASL - getting into the air**

The challenge at this point for the RASL team is to get the instrument into the air for testing under actual flight conditions. The ground-based measurements presented here demonstrate that RASL more than meets the performance expectations indicated by numerical modeling [19]. This implies that it is in fact capable of more than an order of magnitude improvement in water vapor measurements over existing airborne water vapor lidars. For RASL to fly, we

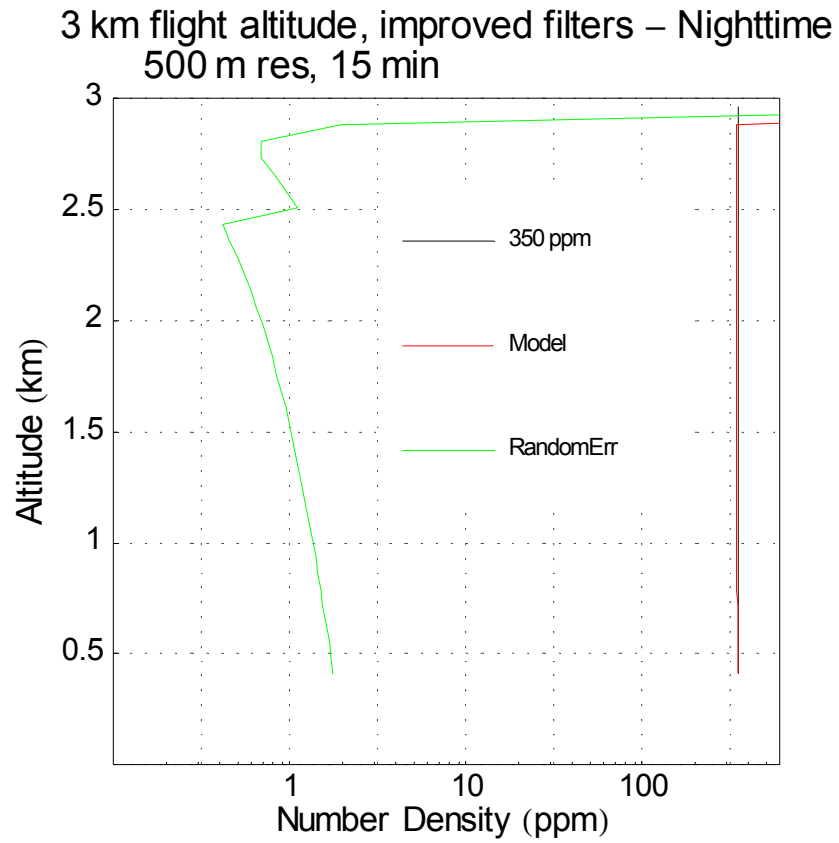


Figure 19: Simulation of RASL measurements of CO<sub>2</sub> from a flight altitude of 5 km. Using a 500 meter vertical resolution, errors range between 1 and 5 ppm from 4 km to the surface.

must first develop two critical feedback systems: one to maintain the laser power as the system undergoes thermal and mechanical variations in flight, the other to maintain the system boresite alignment as these same parameters vary. We must also design and build the RASL frame as well as the aircraft window to accommodate the full 0.6 m aperture of RASL. Up to this point, we have identified a funding source for only the laser power stabilization system (GSFC Technology Transfer Program). That system is now under development. However, there do not appear to be compatible funding sources within NASA to support the development of the other necessary hardware for a full demonstration of RASL. However, if funding can be found to permit RASL to be fully tested in the air, the research completed under this IIP activity indicates that RASL will be able to provide atmospheric measurements of unprecedented resolution and variety that address high priority Earth Science Enterprise objectives.

## 8 References

- [1] S. H. Melfi, D. N. Whiteman, R. A. Ferrare, "Observation of atmospheric fronts using Raman lidar moisture measurements", *J. App. Meteor.*, **28**, 789-806 (1989).
- [2] R. A. Ferrare, Melfi S. H., Whiteman D. N., Evans K. D., "Raman Lidar Measurements of Pinatubo Aerosols over Southeastern Kansas during November - December 1991. *Geophys. Res. Lett.*, 19: (15) 1599-1602 (1992).
- [3] A. J. Behrendt and J. Reichardt, "Atmospheric temperature profiling in the presence of clouds with a pure rotational Raman lidar by use of an interference-filter-based polychromator", *Appl. Opt.*, 39: (9) 1372-1378 (2000).
- [4] D. D. Turner, J. E. M. Goldsmith, "Twenty-four-hour Raman lidar water vapor measurements during the Atmospheric radiation Measurement program's 1996 and 1997 water vapor intensive observation periods", *J. Atmos. Ocean. Tech.*, 16: (8) 1062-1076 (1999).
- [5] D. N. Whiteman, S. H. Melfi, "Cloud liquid water, mean droplet radius and number density measurements using a Raman lidar", *J. Geophys. Res.*, **104**, No. D24, 31411-31419 (1999).
- [6] A. Ansmann, U. Wandinger, M. Riebesell, C. Weitkamp, W. Michaelis, "Independent Measurement of Extinction and Backscatter Profiles in Cirrus Clouds by using a Combined Raman Elastic-Backscatter Lidar", *Appl. Opt.*, 31: (33) 7113-7131 (1992).

- [7] D. N. Whiteman, K. D. Evans, B. Demoz, D. O'C. Starr, D. Tobin, W. Feltz, G. J. Jedlovec, S. I. Gutman, G. K. Schwemmer, M. Cadirola, S. H. Melfi, F. J. Schmidlin, "Raman lidar measurements of water vapor and cirrus clouds during the passage of hurricane Bonnie", *J. Geophys. Res.*, 106, No. D6, 5211-5225 (2001).
- [8] R. A. Ferrare, R. A., S. H. Melfi, D. N. Whiteman, K. D. Evans, R. Leifer, "Raman lidar measurements of aerosol extinction and backscattering 1. Methods and comparisons." *J. Geo. Phys. Res.*, **103**, D16, 19663-19672 (1998).
- [9] B. B. Demoz, D.O'C. Starr, D.N. Whiteman, K.D. Evans, and D. Hlavka, "Raman LIDAR detection of cloud base", *Geophys. Res. Lett.*, Vol 27, No. 13, 1899-1902 (2000).
- [10] D. Muller, K. Franke, F. Wagner, D. Althausen, A. Ansmann, J. Heintzenberg, "Vertical profiling of optical and physical particle properties over the tropical Indian Ocean with six-wavelength lidar 1. Seasonal cycle", *J. Geophys. Res. - Atmos.* 106: (D22) 28567-28575 (2001).
- [11] Berkoff TA, Whiteman DN, Rallison RD, Schwemmer GK, Ramos-Izquierdo L, Plotkin H, "Remote detection of Raman scattering by use of a holographic optical element as a dispersive telescope", *Opt. Lett.*, 25 (16): 1201-1203 AUG 15 2000
- [12] Chin, M., P. Ginoux, S. Kinne, B.N. Holben, B. N. Duncan, R. V. Martin, J. A. Logan, A. Higurashi, T. Nakajima, 2001: Tropospheric aerosol optical thickness from the GOCART model and comparisons with satellite and sunphotometer measurements, submitted to *J. Atmos. Sci.*
- [13] Melfi, S. H., K. D. Evans, J. Li, D. Whiteman, R. Ferrare, G. Schwemmer, "Observation of Raman scattering by cloud droplets in the atmosphere", *Appl. Opt.*, **36**, 15, 3551-3559 (1997)
- [14] Heaps WS, Burris J, French JA, "Lidar technique for remote measurement of temperature by use of vibrational-rotational Raman spectroscopy", *APPLIED OPTICS*, 36 (36): 9402-9405 DEC 20 1997
- [15] Rizi, V., et. al., Raman Lidar for measurement of cloud liquid water, proceedings of the 21st International Laser Radar Conference, Quebec City, Canada (2002).
- [16] Whiteman, David N., George E. Walrafen, Wen-Huang Yang, S. Harvey Melfi, 1999: Measurement of an isosbestic point in the Raman spectrum of liquid water by use of a backscattering geometry, *Appl. Opt.* 38, 2614-2615
- [17] Whiteman, D. N., S. H. Melfi, "Cloud liquid water, mean droplet radius and number density measurements using a Raman lidar", *J. Geophys. Res.*, Vol 104 No. D24, 31411-31419 (1999)

- [18] D. N. Whiteman, T. Berkoff, D. Turner, T. Tooman, R. Ferrare, L. Heilman, "Research efforts in the absolute calibration of a Raman water vapor lidar", presented at the 20th International Laser Radar Conference, Vichy, France, July 2000.
- [19] Whiteman, D. N., G. Schwemmer, T. Berkoff, H. Plotkin, L. Ramos-Izquierdo, G. Pappalardo, "Performance modeling of an airborne Raman water-vapor lidar", *Appl. Opt.* 40, 375-390 (2001)
- [20] Whiteman, D. N., K. D. Evans, B. Demoz, D. O'C. Starr, E. W. Eloranta, D. Tobin, W. Feltz, G. J. Jedlovec, S. I. Gutman, G. K. Schwemmer, M. Cadirola, S. H. Melfi, and F. J. Schmidlin, "Raman lidar measurements of water vapor and cirrus clouds during the passage of Hurricane Bonnie", *J. Geophys. Res.*, Vol. 106, No D6, 5211-5225 (2001).
- [21] D. Muller, D., K. Franke, F. Wagner, D. Althausen, A. Ansmann, J. Heintzenberg, G. Verver, "Vertical profiling of optical and physical particle properties over the tropical Indian Ocean with six-wavelength lidar 2. Case studies", *J. Geophys. Res. - Atmos.* 106: (D22) 28577-28595 (2001).